COMPARISON OF THE LAYER STRUCTURE OF VAPOR PHASE AND LEACHED SRL GLASS BY USE OF AEM

BRUCE M. BIWER,* JOHN K. BATES,* TEOFILO A. ABRAJANO, Jr.,* AND JOHN P. BRADLEY**
*Argonne National Laboratory, 9700 South Cass Avenue, Argonne, IL 60439
**McCrone Environmental Services, Inc., 850 Pasquinelli Drive, Westmont, IL 60559

CONF-891119--106

DE90 007789

ABSTRACT

Test samples of 131 type glass that have been reacted for extended time periods in water vapor atmospheres of different relative humidities and in static leaching solution have been examined to characterize the reaction products. Analytical electron microscopy (AEM) was used to characterize the leached samples, and a complicated layer structure was revealed, consisting of phases that precipitate from solution and also form within the residual glass layer. The precipitated phases include birnessite, saponite, and an iron species, while the intralayer phases include the U-Ti containing phase brannerite distributed within a matrix consisting of bands of an Fe rich montmorillonite clay. Comparison is made between samples leached at 40°C for 4 years with those leached at 90°C for 3-1/2 years. The samples reacted in water vapor were examined with scanning electron microscopy and show increasing reaction as both the relative humidity and time of reaction increases. These samples also contain a layered structure with reaction products on the glass surface.

INTRODUCTION

The ability to understand and model the reaction of nuclear waste glasses under conditions relevant to those expected at the proposed Yucca Mountain repository site requires a complete description of the reacted glass. The identification of stable secondary phases, whether formed on the surface of the glass or as an in-situ rearrangement of products of the reacted glass layer, is essential because it is these secondary phases that set the solution saturation levels of all elements, and in essence are the driving force of continued glass reaction [1]. In the unsaturated environment expected at the tuff repository, glass will be exposed to water vapor and subsequently may be contacted by small amounts of standing water. To study the behavior of glasses under both conditions, long-term tests have been performed by Westinghouse Savannah River Company (WSRC) and by the Yucca Mountain Project (YMP). Tests of long duration are of interest because they allow for the greatest degree of alteration.

In this report we examine the reaction of 131 type glass with water vapor and liquid water. This glass was chosen because samples from long-term vapor hydration and static leach tests are available, and because the results from the leach tests have been used in developing models [1,2] to predict glass performance. While the composition of the 131 glass samples examined is not expected to be used for glasses produced in the Defense Waste Processing Facility (DWPF), it is possible that glasses of similar durability may be manufactured. Thus, experience gained in studying the alteration processes of this glass is likely to be transferable to the study of more durable glasses.

EXPERIMENTAL

Leach Samples

The glasses examined were taken from a study performed by WRSC [3]. One sample had been reacted for 1274 days (1274D) in deionized water at 90°C following the MCC-1 procedure. The second sample had been reacted for 1456 days (1456D) at 40°C. The glass composition (Glass I) and details of the experimental procedures are provided by Wicks [3]. After the tests were completed, the leaching data were tabulated and the glass samples were retained in storage.

Vapor Samples

The 131 type glass used in the vapor studies [4] came from a different batch (Glass II) than was used by Wicks. The main differences in composition (elemental wt %) between Glass I/Glass II are in uranium (0.88/0.0) and aluminum (2.87/1.72). All of the vapor tests were conducted at 75°C with relative humidities (RH) of 60% (365D), 95% (365D, 731D), and 100% (365D). These humidities were chosen because during the containment period in the repository, the temperature differential between the waste and the rock will be small such that a two-phase (liquid + vapor) system will exist in the tuff surrounding the waste package. The RH in the air gap will be established by the temperature differential, and calculations [5] indicate the RH may range between 60 and 100% during containment. The humidities were also chosen because the rate of glass reaction below 60% RH is very slow, being limited by the small amount of liquid water that sorbs to the glass surface [6].

The 60% RH test was conducted in a Blue M bell jar. A drip cap was located above the sample to keep any condensed liquid from contacting the glass. The 95% RH samples were hydrated in a Blue M environmental chamber where the water condensation problem was eliminated by the chamber design. The 100% RH sample was contained in an individual Teflon™ vessel, the sample being supported on a Teflon™ grid over liquid water. The Teflon™ vessel was placed in the environmental chamber to reduce water loss from the vessel. No drip diverter was used, and the sample likely was contacted by dripping water sometime during the reaction period.

ANALYSES

Leached Samples

The leached samples were first examined with optical microscopy (OM), were then mounted in resin and cross-sectioned for examination using scanning electron microscopy/energy dispersive spectroscopy (SEM/EDS), and finally were thin-sectioned and examined with AEM. The thin-sections were prepared using an ultramicrotome equipped with a diamond knife. We employed an ultramicrotomy procedure developed specifically for preparation of micrometer-sized geochemical specimens for electron microscopy studies [7,8]. Application of these procedures enabled us to prepare, under ambient conditions, electron transparent sections (50-100 nm thick) of the reacted layers with minimal disturbance of their microstructures and indigenous petrography. Thin-sections were examined in a 200 keV analytical electron microscope, using lattice fringe imaging, electron micro-diffraction, and quantitative thin-film x-ray analysis [9,10]. AEM data acquisition was complicated by overall poor crystallinity within the reacted layers, fine scale intercalation of phases, and sensitivity of some

phases, particularly the layer silicates, to electron irradiation damage. A liquid nitrogen cooled cold stage was used to minimize irradiation damage and specimen contamination from the microscope itself.

Sample 1274D had a surface that was marked by distinct orange swirls punctuating the black background of the glass. These swirls were formed as the glass was cast. The reacted surface was covered by a white haze and spotty clusters of discrete fibrous islands, and was very friable.

An overview of the ordering of the precipitated phases and the residual layer for 1274D is shown in Fig. 1. The layer is non-uniform in both thickness and structure as it encompasses the sample. The layer thickness ranges from 20-40 μm, while the structure varies, having 8 to 16 discrete sublayers. The original glass surface is marked by the dark stain (Fig. 1a) which is composed of noncrystalline Fe. Above the stain are layers 1 and 2 (Fig. 1a) which are a mixture of birnessite ($Mn_7O_{13}\cdot 5H_2O$) and the Mg-rich clay saponite $(Mg,Al,Ni)_3\ (Al,Si)_4\ O_{10}(OH)_2$. Layer 1 makes up the fibrous islands and contains most of the birnessite. Layer 2 forms a vertically oriented band over the entire surface, and while containing some birnessite is comprised mainly of saponite. The phases were identified based on composition, lattice imaging, and microdiffraction.

Below the Fe stain is a repeating layer structure of fine-grained, randomly oriented crystals alternating with open bands of well-ordered vertically oriented single sheets (layers 3-6 in Fig. 1b). Depending on the location on the sample, this alternating structure repeats itself up to five times. The composition of both types of bands are similar, having a cation to silica ratio of 1.40; major element composition in normalized atom % of Si-41.5, Mg-8.6, Al-26.5, Fe-19.8, Ni-3.5; a basal spacing based on lattice imaging of between 10-13.5 Å; and a microdiffraction pattern that matched that of smectite. The bands consisted of only one crystalline phase, which based on the above information is tentatively assigned as a Fe-rich montmorillonite clay.

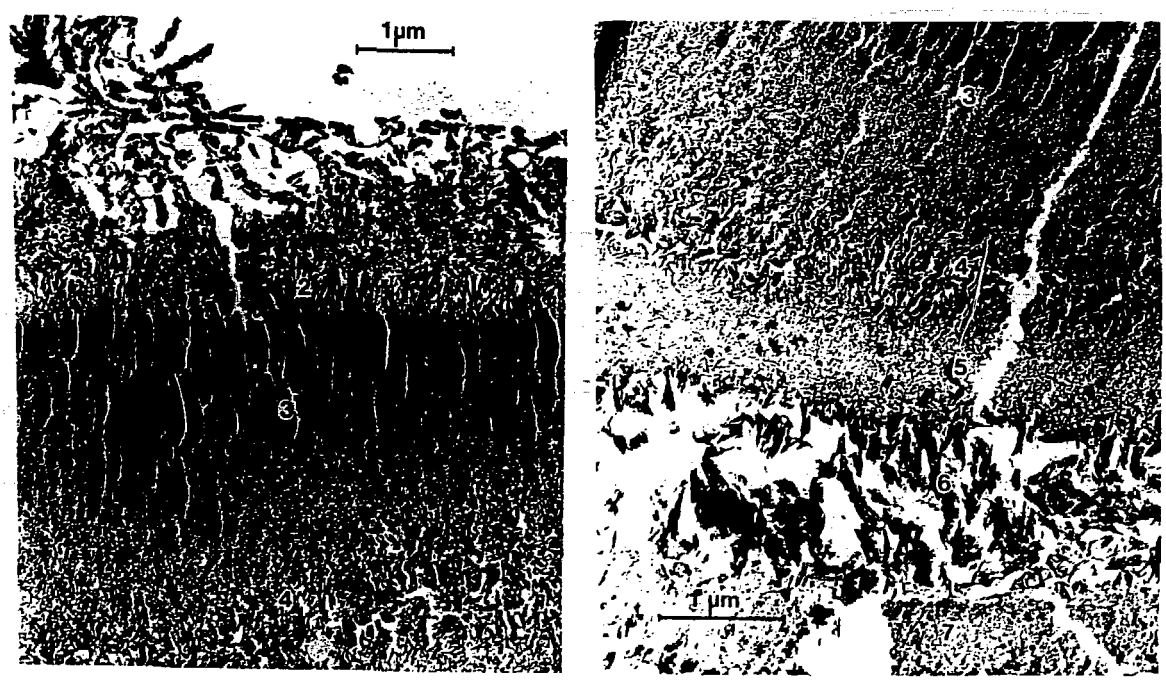

(a) (b)

Figure 1. Brightfield Transmitted Image of Ultramicrotomed Thin-Sections of Sample 1274D. (a) Layers 1-4, (b) Layers 3-7.

Interspersed in all the layers, from the surface inward, are inclusions of a U-Ti bearing phase, presumably an oxide or hydroxide based on EDS analysis (Fig. 2). Since these inclusions were poorly crystalline aggregates of nanometer-sized grains, it was not possible to directly obtain interpretable crystal structure data. A naturally occurring analogue to the inclusions is probably brannerite, a U-Ti oxide, which in its native state is usually metamict or non-crystalline [11].

Finally, as the layer structure approaches the base glass, the degree of ordering decreases until the microdiffraction pattern of the layer matches that of the glass. This inner layer, which ranges in thickness up to 4 μm, is completely depleted in Li, B, and Na, and partially depleted in Mn, but otherwise retains its original glass-like composition.

The appearance of the entire layer for sample 1456D reacted at 40°C, is nearly identical to that described above for the inner layer of 1274D (Fig. 3). The layer ranges between 1 and 4 μm thick, depending on the extent that cracks penetrate into the glass. The cracks are demarkated by deposits of the Fe-rich stain, which for this sample are crystalline and have been identified as magnetite. The Fe stain does not trace the entire surface (Fig. 3), and there are concentrations of U and Ti near the surface that can be detected with EDS. No phases are observed to have precipitated onto the surface, nor has the layer restructured such that discrete phases can be identified.

Vapor Samples

The vapor samples were examined with OM, SEM/EDS, and secondary ion mass spectroscopy (SIMS), and the secondary phases were identified with X-ray diffraction (XRD). Thin-sectioning and analysis of these samples with AEM is currently in progress. Sample 365D (60% RH) was covered with a light haze. The thickness of the reacted layer, as determined by Li, B, and Na depletion (SIMS), was 750 Å. The surface of the sample retained the smooth appearance of non-reacted glass, and the major secondary phases identified were NaCl and a Na-S rich phase.

Sample 365D (95% RH) was noticeably reacted. The surface had begun to develop an open pore or cross-hatched structure, and phases that formed on the surface were identified by XRD to be smectite and calcite. The same Na-rich phases as noted for sample 365D (60% RH) were present, but were not as pervasive as on the low humidity sample. In cross-section, the reacted layer was determined to be ~5 μm thick. The reacted layer was depleted in B, Li, and Na, while the near-surface region was enriched in Mn, Ni, and Si.

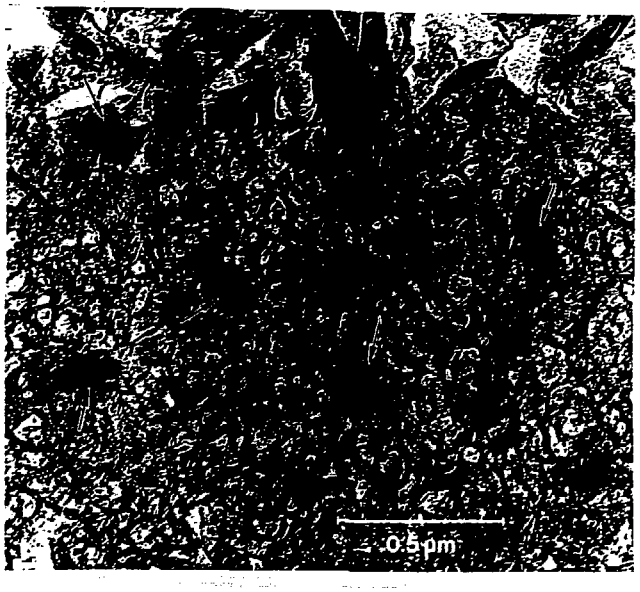

Figure 2
Brightfield Image of an Inclusion of a U-Ti Phase Interspersed Among the Randomly Oriented Crystals in Layer 3 of Sample 1274D.

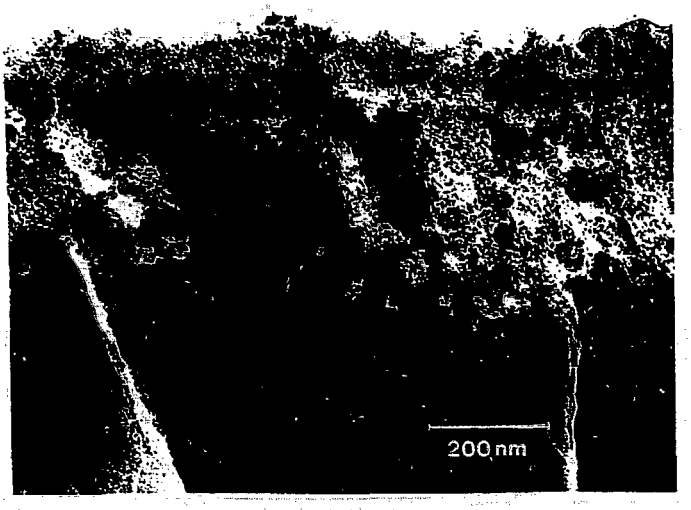

Figure 3
Brightfield Image of the Entire Layer from Sample 1456D.

After 761D at 95% RH, the glass was even more reacted (Fig. 4). Two discrete secondary phases were identified as analcime and calcite (Fig. 4) and the reacted layer was ~7 μm thick. The cross-sectional elemental profiles are the same as for 365D (95% RH), depleted in B and Na, with enrichment of Ni, Mn, and Si in the near-surface area. The appearance of analcime is significant in that it is the first phase to form in vapor reaction at higher temperatures. At 200°C analcime formation begins after one day of reaction.

The sample reacted at 100% RH for 365D was the most altered of the vapor samples. The surface was covered with extensive mats or islands of a white patchy material identified as smectite. The reacted layer ranged in thickness from 15 to 35 μm, and had the banded sublayer structure shown in Fig. 5a. The layer is depleted in B and Na (Li was not profiled), while the remaining elements had the profiles shown in Fig. 5b. Identification of the phases formed by restructuring of the reacted layer will be determined by AEM. No Na-rich phases were found on the surface, probably because of the possibility of dripping water noted previously.

DISCUSSION

The structure of the leached sample, 1274D (Glass I), will be compared initially with that of Glass II leached at 90°C for 546 days following the MCC-1 format. Results from the Glass II leaching experiments have been presented previously [12]. The precipitated phases for both glasses were birnessite, saponite, and iron; the morphology (islands and a vertical layer) were also the same. However, the phase segregation was less complete, and the island coverage less pervasive in 1274D. The Fe stain was non-crystalline in the 1274D and 546D samples, but for the shorter term (28D) leached Glass II sample, the iron existed as magnetite and iron metal.

The residual layers showed less similarity. Both glasses showed a layered structure of fine- and coarse-grained crystals. However, for Glass II the layer structure was consistent throughout the entire sample, and there was only one coarse-grained band. This band had the appearance of layer 4 for Glass I (Fig. 1a) and was composed of a mixture of an iron-rich smectite and serpentine. The mineral phases for Glass II were not Al-rich (as was observed for Glass I) and the coarse-grained band has a total cation to silicon ratio between 0.9 and 1.2, which is intermediate between smectite and serpentine. No vertically ordered open bands were noted for Glass II, and the Glass II surface layer remained intact with the glass even five years after leaching was completed. Glass II also had an inner

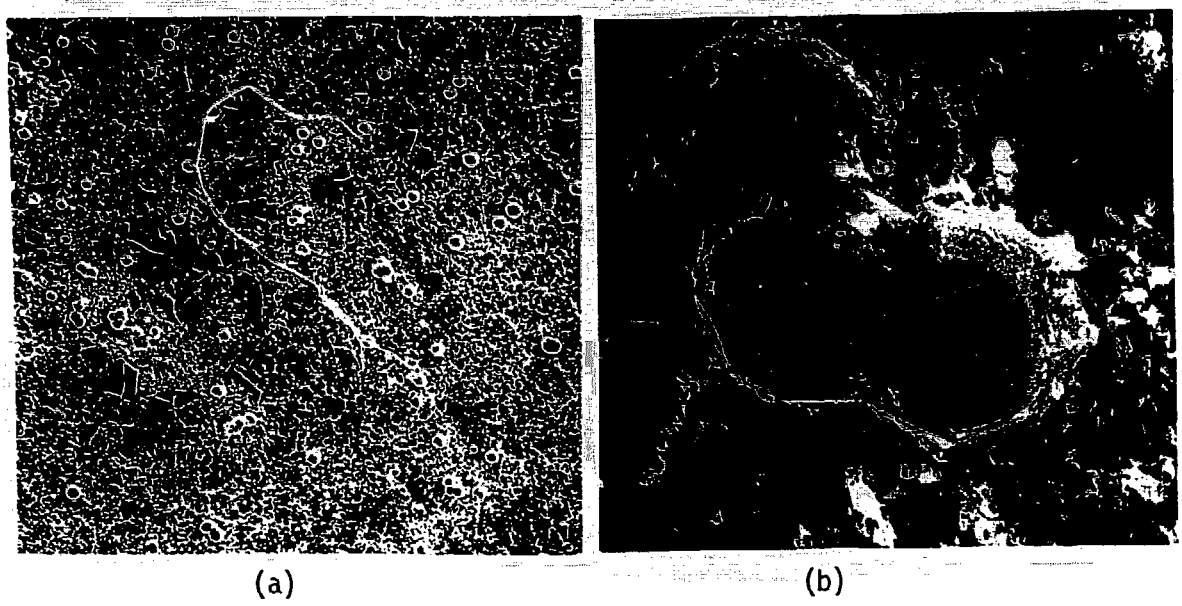

(a) (b)

Figure 4. (a) Photomicrograph of the Reacted Surface of Sample 761D (95% RH), Magnification = 100X; and (b) Photomicrograph of Analcime Phases that Form on the Surface of 761D (95% RH), Magnification = 2000X.

layer next to the bulk glass that was glass-like in structure and Si composition. Of course, Glass II had no U-Ti phase, but also showed no distinct Ti segregation. Finally, the leachate results from both glasses compared as normalized elemental mass losses, were the same for both glasses as a function of time.

Thus, although the leachate results for the two glasses are similar, the physical integrity and structure of the residual layer are considerably different. That the phases precipitated from solution are the same is reasonable since the leachates have similar compositions. The differences in the residual layers is noteworthy, especially the Al-rich nature of the phases in Glass I, and the open banding in Glass I which is likely the reason for its poor-structural stability.

Two observations related to Glass I are worth extra note. The formation of an actinide-bearing phase within the reacted layers is extremely significant because it reveals that radionuclide release can be retarded even though the glass may continue to react. The leachate results from sample 1274D indicate the uranium was released from the glass at a rate 7-20 times lower than boron depending on the leaching time [3]. This is surprising when compared to uranium release previously observed in other more durable nuclear waste glasses, where boron and uranium were released to the solution according to their stoichiometric proportions in the glass [13]. The second observation, the lack of structural rigidity in the layer, is important because under potential dripping water contact modes expected for the YMP site, exfoliation of surface layers from the glass has been identified as an important factor in increasing release rates [14].

The reaction of Glass I at 40°C may help elucidate the short- and long-term reaction processes at 90°C. The appearance, structure, and composition of the 1456D layer provides insight as to its formation. The layer retains its glass-like composition except for deletion of B, Na, and Li, shows no evidence of restructuring into crystalline phases, and forms a diffuse boundary with the unreacted glass. This suggests the structure of the glass remains intact as elements are leached from the glass and the layer forms. There is no evidence for stoichiometric dissolution of the

(a)

(b)

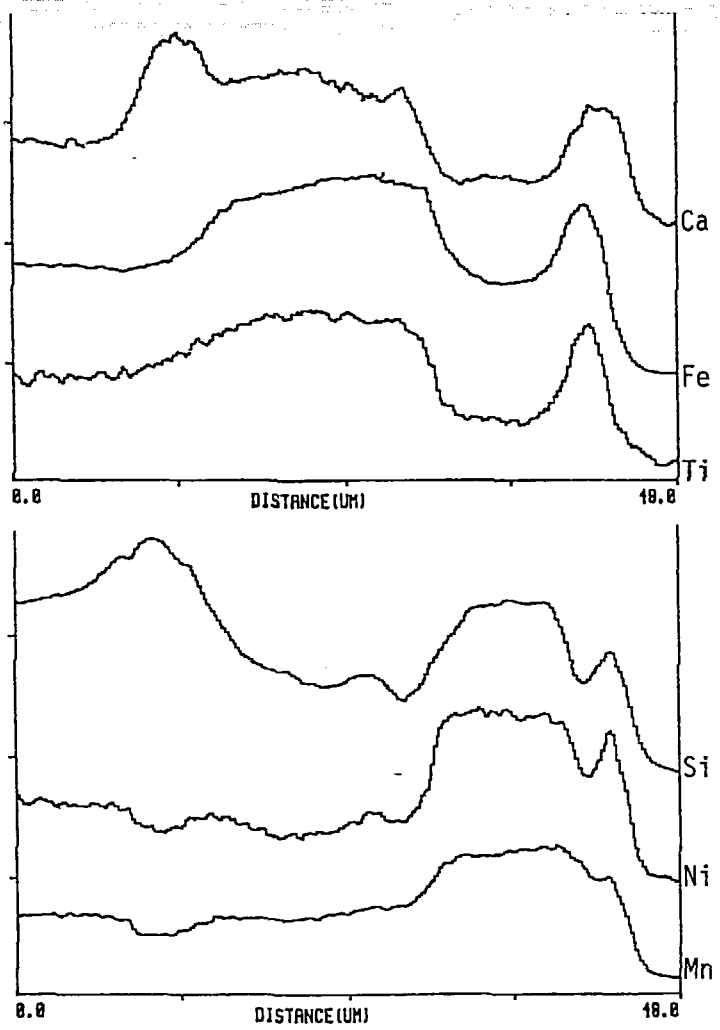

Figure 5. (a) Cross-Section of Sample 365D (100% RH) Showing the Bonded Layer Structure and (b) Elemental Profiles Across the Reacted Layer. Magnification = 2000X.

glass. The relationship to the long-term 90°C leach tests is in comparison with the inner layer, whose characteristics are similar to those just described. While 1274D has undergone restructuring of the intermediate layers, indicating the silicate network has been completely hydrolyzed, the restructuring does not occur at the layer/glass interface, but at the nebulous boundary between the inner layer and the crystalline bands.

The present vapor tests indicate that at 75°C, the extent of reaction increases significantly as the RH is increased from 60 to 100% RH. The layer thickness observed at 100% RH after one year, ~35 μm, is of the same order as observed for Glass I leached in a static solution for 1274 days at 90°C. The precipitates formed in the vapor tests include Na-rich phases on a surface that have transformed into smectite. A segregation of Mn and Ni to the near-surface region may result in the formation of the birnessite as observed in the leaching tests. Additional AEM analyses will clarify this point.

In the vapor tests, the glass reaction is initiated by a thin film of water that sorbs onto the glass surface [15]. The reaction proceeds as a hydrated layer forms in combination with the nucleation of secondary phases on the glass surface. The secondary phases act as sinks to incorporate elements that are "leached" from the glass, while the ingress of water and the depletion of "leached" elements defines the extent of reaction. Thus, whereas the reaction progress in the leach tests slows due to the saturation of the leachate, the vapor tests continue to react as the secondary phases form.

CONCLUSIONS

Glass samples reacted under liquid and vapor conditions for time periods up to four years have been examined using AEM and other surface analytical techniques. The samples reacted in liquid at 90°C have formed secondary phases precipitated from solution and crystallized within the residual layer. The vapor phase samples exhibited a layer structure similar to that observed on the leached samples. Elements "leached" from the vapor phase samples collect in secondary phases on the sample surface rather than dissolving in solution, simply an extreme case of a large surface area to volume ratio. Finally, small variations in glass composition were shown to have a significant affect on the reacted layer development.

ACKNOWLEDGMENTS

Work supported by the U.S. Department of Energy, Office of Civilian Radioactive Waste Management, Yucca Mountain Project under subcontract to Lawrence Livermore National Laboratory, SANL 810-007, and the Office of Defense Programs under Contract Number W-31-109-Eng-38.

REFERENCES

1. W. L. Bourcier, "Geochemical Modeling of Radioactive Waste Glass," Lawrence Livermore National Laboratory report UCRL-57012, in press.
2. B. Grambow, in Scientific Basis for Nuclear Waste Management VIII (C. M. Jantzen, J. A. Stone, and R. C. Ewing, eds.) 15 (1985).
3. G. G. Wicks, J. A. Stone, G. T. Chandler, and S. Williams, "Long-Term Leaching Behavior of Simulated, Savannah River Plant Waste Glass," E.I. du Pont de Nemours Co., Savannah River Laboratory DP-1728 (1986).
4. J. K. Bates, D. J. Lam, and M. J. Steindler, in Scientific Basis for Nuclear Waste Management VI (D. Brookins, ed.) 6 (1983).

5. J. K. Bates, et.al., Lawrence Livermore National Laboratory, report UCRL-15801-86-1 (1987).
6. W. L. Ebert and J. K. Bates, "The Reaction of Synthetic Nuclear Waste Glass in Steam and Hydrothermal Solution," This Volume (1989).
7. J. P. Bradley and D. E. Brownlee, Science 231, 889 (1986).
8. J. P. Bradley, Geochim. Cosmochim. Acta 52, 889 (1988).
9. G. Cliff and G. W. Lorimer, J. Microsc. 103 (1975).
10. P. Sheridan, J. Electron Microsc. Tech. 11, 41 (1989).
11. A. Pabst, Am. Min. 39, 109 (1954).
12. T. A. Abrajano, Jr., J. K. Bates, and J. P. Bradley, "Analytical Electron Microscopy of Leached Nuclear Waste Glasses," presented at the Am. Ceram. Soc. Mtg., Indianapolis, IN, April 1989.
13. W. L. Ebert, J. K. Bates, and T. J. Gerding, "The Reaction of Glass During Gamma Irradiation in a Saturated Tuff Environment, Part 4: SRL 165, ATM-1c, and ATM-8 Glasses at 1E3 R/h and 0 R/h," Argonne National Laboratory Report (in press).
14. J. K. Bates, T. J. Gerding, A. B. Woodland, "Parametric Effects of Glass Reaction Under Unsaturated Conditions," (This Volume) (1989).
15. T. A. Abrajano, Jr., J. K. Bates, and J. J. Mazer, "Aqueous Corrosion of Natural and Nuclear Waste Glasses. II. Mechanisms of Vapor Hydration of Nuclear Waste Glasses," J. Non-Cryst. Sol. 108, 269-288 (1989).

DISCLAIMER